J Mol Model (2008) 14:957–966
DOI 10.1007/s00894-008-0342-8

ORIGINAL PAPER

Computational studies of the binding site of α_{1A}-adrenoceptor antagonists

Minyong Li · Hao Fang · Lupei Du · Lin Xia · Binghe Wang

Received: 26 February 2008 / Accepted: 18 June 2008 / Published online: 15 July 2008

Abstract Aimed at achieving a good understanding of the 3-dimensional structures of human α_{1A}-adrenoceptor (α_{1A}-AR), we have successfully developed its homology model based on the crystal structure of β_2-AR. Subsequent structural refinements were performed to mimic the receptor's natural membrane environment by using molecular mechanics (MM) and molecular dynamics (MD) simulations in the GBSW implicit membrane model. Through molecular docking and further simulations, possible binding modes of subtype-selective α_{1A}-AR antagonists, Silodosin, RWJ-69736 and (+)SNAP-7915, were examined. Results of the modeling and docking studies are qualitatively consistent with available experimental data from mutagenesis studies. The homology model built should be very useful for designing more potent subtype-selective α_{1A}-AR antagonists and for guiding further mutagenesis studies.

Keywords α_{1A}-Adrenoceptor (α_{1A}-AR) · β_2-Adrenoceptor (β_2-AR) · Antagonists · Homology modeling · Molecular docking · Molecular dynamics (MD) · Molecular mechanics (MM)

M. Li (✉) · L. Du · B. Wang (✉)
Department of Chemistry and Center for Biotechnology and Drug Design, Georgia State University, Atlanta, GA 30302, USA
e-mail: mli@gsu.edu
e-mail: wang@gsu.edu

H. Fang · B. Wang
Department of Medicinal Chemistry, Shandong University, Jinan, Shandong 250012, China

L. Xia
Department of Medicinal Chemistry, China Pharmaceutical University, Nanjing, Jiangsu 210009, China

Introduction

As crucial members of the G-protein coupled receptor (GPCR) superfamily, α_1-adrenoceptors (α_1-ARs) are known to mediate the actions of endogenous catecholamines such as norepinephrine and epinephrine [1, 2]. Pharmacological evidence and recent molecular cloning studies have demonstrated that α_1-ARs are not a homogeneous population. Three distinct α_1-AR subtypes, α_{1A}, α_{1B} and α_{1D}, have been characterized by functional analysis, radio-ligand binding and molecular biology studies [3]. Among these three subtypes, α_{1A}-AR controls prostate smooth muscle tone in human and is regarded as a target for the treatment of benign prostate hyperplasia (BPH) [4, 5]. We have had a long-standing interest in the development of α_1-AR antagonists for various applications [6–13]. However, the lack of detailed structural information of α_{1A}-AR is a major hindrance in our effort to search for potent and selective α_{1A}-AR antagonists. Several homology models for human α_{1A}-AR, including one from ourselves [7], have been reported. However, these homology models were all based on the crystal structure of a light activated GPCR, bovine rhodopsin [14–16], with which the human α_{1A}-AR shares only 21% sequence identity. Since the commonly accepted threshold of sequence identity for accurate homology modeling is about 25% [17], the low sequence identity between bovine rhodopsin and human α_{1A}-AR most likely have led to significant inaccuracies of the resulting homology models.

Recently, three exciting papers by the Kobilka group [18–20] at the end of 2007 described the crystal structure of a closely related adrenoceptor: β_2-adrenoceptor (β_2-AR), which is also a GPCR. These β_2-AR structures, together with the existing structures of rhodopsin, represent monumental steps in understanding how GPCRs work at the molecular level [21]. β_2-AR and α_{1A}-AR belong to the same family of adrenoceptors and share a modest degree of

sequence identity (36%). Therefore, the availability of the β_2-AR crystal structure gives an excellent opportunity to develop an α_{1A}-AR homology model with improved accuracy when compared with earlier reported models. Herein we describe our effort in building and optimizing an α_{1A}-AR homology model. The quality of this model was examined by using computational methods and by comparing the computational results of docked known antagonists with results from mutagenesis studies.

Materials and methods

Homology modeling

The construction of the α_{1A}-AR homology model followed a series of well-defined and commonly accepted steps: 1) sequence alignment between the target and the template; 2) building an initial model; 3) refining the model; and 4) evaluating the quality of the model [22]. In the current homology modeling effort, the crystal structure of human β_2-AR (PDB entry: 2R4R) at 2.4 Å resolution was chosen as the template. The sequence of human α_{1A}-AR was retrieved from Swiss-Prot database (accession number P35348, entry name ADA1A_HUMAN) and aligned with human β_2-AR using the T-Coffee multiple alignment program [23] and the ESPript program [24] (Fig. 1). Then, the homology model of α_{1A}-AR was constructed using MODELLER 9v2 with default parameters [25].

Refinement of the homology model

MD simulations were carried out by using the CHARMM c33b1 program [26] and an implicit membrane model, GBSW (Generalized Born model with a simple Switching function) [27]. The protein atoms were parameterized by CHARMM-GUI [28] using the CHARMM22 force field [29]. The surface tension coefficient (representing the non-polar solvation energy) was set to 0.03 kcal/(mol·Å^2), which was consistent with literature precedents in the calculation of non-polar contributions in soluble proteins [27]. The

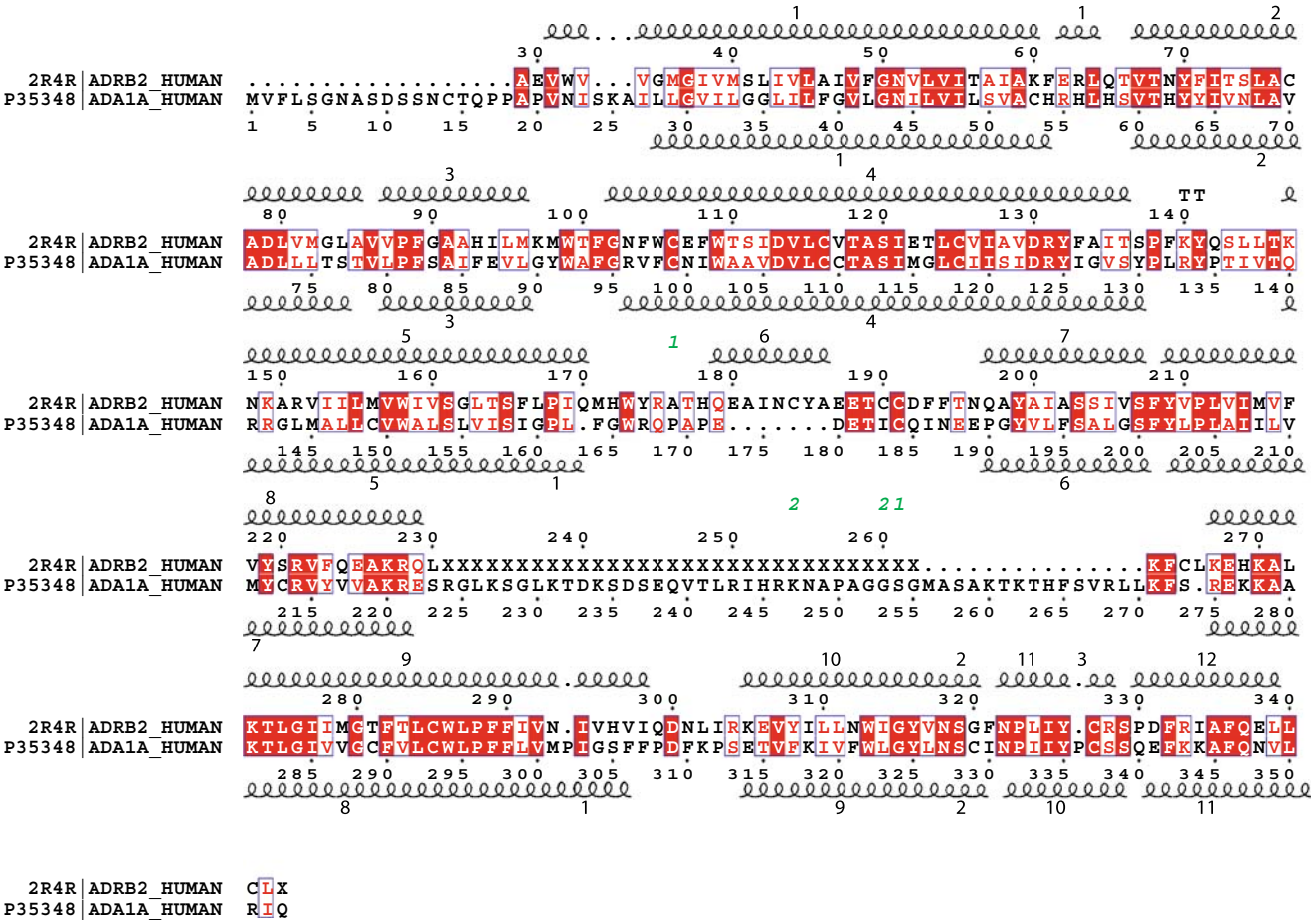

Fig. 1 Secondary structure-based sequence alignment of human α_{1A} and β_2-AR

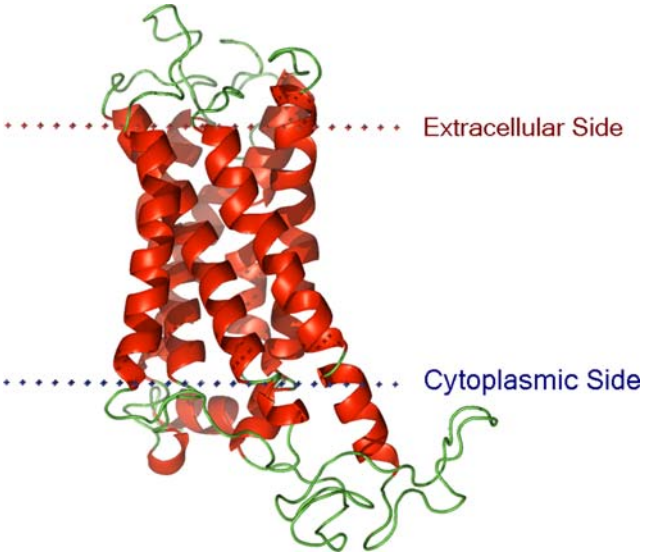

Fig. 2 Initial conformation of α_{1A}-AR in the GBSW implicit membrane model

membrane thickness centered at Z=0 was set to 30.0 Å with a membrane smoothing length of 5.0 Å (w_m=2.5 Å) (Fig. 2). Such implicit membrane settings are consistent with the commonly believed membrane environment [27]. All bond lengths involving hydrogen atoms were fixed using the SHAKE algorithm [30]. No cutoff for the non-bonded and GB energy calculations was used. Simulation temperature was at 300 K. Minimizations were carried out using 1500 steps of steepest descent, followed by Adopted Basis Newton-Raphson (ABNR) minimization until the root mean square gradient was less than 0.001 kcal/mol Å. The whole system was then equilibrated for 50 ps, followed by another 10 ns of canonical ensemble (NVT)-MD simulation run.

Assessment of the homology model

In homology modeling, it is very important that appropriate steps are built into the process to assess the quality of the model [31]. Therefore, the geometric quality of the backbone conformation and the appropriateness of residue interactions, residue contacts, and energy profiles of the homology model were assessed using PROCHECK [32], ERRAT [33], VERIFY-3D [34], WHAT-IF [35] and DOPE [36]. Such practice is the same as what we have used in the past with other homology models [37–40].

Validation of the homology model by molecular docking

The ability to predict the correct ligand binding poses using the homology model built is an important test. Therefore, the binding modes of three subtype-selective α_{1A}-AR antagonists, Silodosin [41], RWJ-69736 [42] and (+)SNAP-7915 [43] were examined and compared with available experimental data from mutagenesis studies (Fig. 3).

The 3D structures for these three ligands were refined using the PM3 method in the MOPAC 7 program [44] and assigned with AM1-BCC partial charges [45–47] by the QuACPAC program. All partial charges on the atoms of the homology model were derived from AMBER 8 parameters. Docking of the ligands into α_{1A}-AR was performed by using DOCK 5.4 [48]. The active site included residues Ser83, Trp102, Asp106, Val107, Cys110, Tyr111, Ile157, Ser158, Ile178, Tyr184, Ala189, Ser188 Ser192 Phe193, Phe288, Phe289, Phe308, Phe309, Phe312 and Tyr316. After docking, MD simulations were conducted with the ligand-receptor complexes using the same protocol as depicted in the homology model refinement section. Then the ligand-receptor complexes were analyzed by HBPLUS 3.06 [49], LIGPLOT 4.22 [50] and Pymol 0.99 [51].

Hardware and software

Homology modeling, PROSA2003 analysis, DOPE analysis (MODELLER 9v2), binding analysis (HBPLUS 3.06 and Ligplot 4.22) and visualization (PyMOL 0.99) were carried out on a Xeon-based Linux workstation. MM calculations and MD simulations (CHARMM c33b1) were performed on URSA, a 160-processor computer based on the Power5+ processor and IBM's P series architecture. PROCHECK and ERRAT (http://nihserver.mbi.ucla.edu/SAVS/), and WHAT-IF (http://swift.cmbi.ru.nl/servers/html/index.html) validations were computed on-line.

Fig. 3 Chemical structures of Silodosin, RWJ-69736 and (+)SNAP-7915

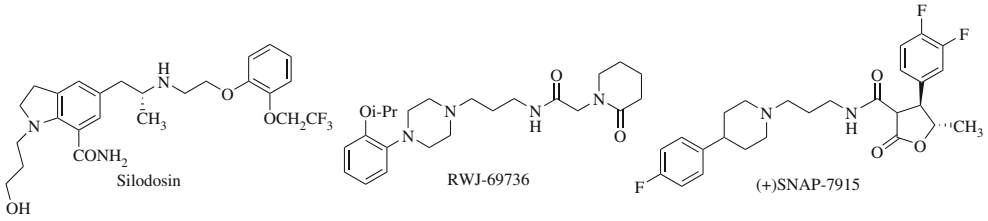

Results and discussion

Again, in our effort of developing α_1-AR antagonists [6–13] we were in need of a high quality 3D model of α_{1A}-AR to guide our medicinal chemistry work. In the absence of an experimentally determined crystal structure, homology modeling provides a rational approach to obtain a reasonable 3D model [52, 53]. It should be noted that homology modeling is currently the most accurate method for the prediction of protein 3-D structures, yielding models suitable for a wide range of applications including structure-based drug design and mechanistic investigations [54, 55]. This approach has been successfully used in building reasonable structural models of membrane proteins when there is an experimentally determined template structure sharing more than 25% sequence identity [17, 56]. Our aim was to build a high quality homology model of α_{1A}-AR to guide our (and other's) medicinal chemistry work by taking advantage of the newly published crystal structure of β_2-AR.

The final sequence and structural alignment of α_{1A}-AR and β_2-AR (Fig. 1) shows about 36% sequence identity. In addition, the root-mean-square deviation (RMSD, Å) between the backbone atoms of the template and the initial rough homology model was only 2.75 Å, which indicated a reasonable model for further MM and MD calculations (Fig. 4).

It is well known that traditional MD simulations in vacuum can severely distort loop structures, especially for membrane proteins [57]. Therefore, we conducted MD simulations using an embedded membrane model [58]. During the MD simulation, the RMSD values of the α_{1A}-AR backbone atoms and all heavy atoms in whole system, and backbone atoms in active site relative to the initial homology model are plotted as time-dependent functions in Fig. 5. The RMSD values of backbone atoms and all heavy atoms in the whole system, and backbone atoms in active site tends to be convergent after 7 ns with fluctuations around 3 Å, 5 Å and 1.8 Å, respectively. Such evidence indicates that the system is stable and has been equilibrated. This optimized homology model has been deposited in Protein Model DataBase (PMDB entry: PM0075211).

Fig. 4 The superposition of β_2-AR crystal structure (gold ribbons) and α_{1A}-AR homology model (blue ribbons)

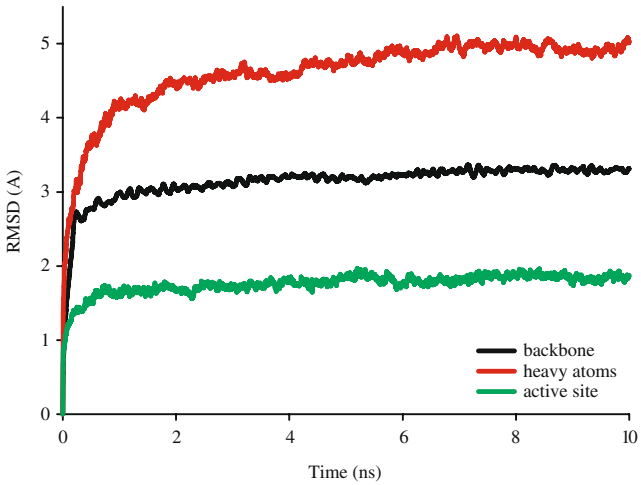

Fig. 5 Time dependence of the RMSD (Å) from α_{1A}-AR homology model for the backbone atoms in a 10 ns MD simulation

The quality profiles of the refined model including the geometric properties of the backbone conformations and the appropriateness of residue interactions and energy profiles were assessed by using PROCHECK, ERRAT, WHAT-IF, PROSA2003 and DOPE. These are the same methods that we have used in previously published studies [37–40]. The results of all these evaluations suggest that a high quality homology model for α_{1A}-AR was obtained.

The first validation carried out here was Ramachandran's plot calculations in PROCHECK program by assessing the stereochemical quality of a given protein structure [32]. The PROCHECK results are summarized in Table 1 and Fig. 6.

Table 1 Quality of structures checked by PROCHECK and ERRAT

	Ramachandran plot quality in PROCHECK*				ERRAT score
	Core	Allowed	General	Disallowed	
Model	89.8	7.7	2.1	0.4	83.2
Template	94.2	5.4	0.4	0.0	96.7

*Ramachandran plot qualities show the percentage (%) of residues belonging to the core, allowed, generally allowed, and disallowed region of the plot.

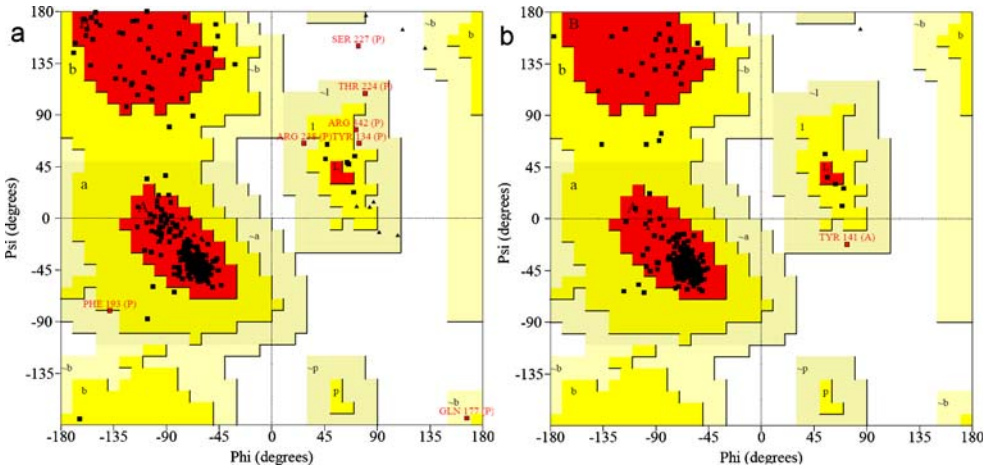

Fig. 6 Ramachandran maps: (**a**) α_{1A}-AR homology model and (**b**) β_2-AR template

Altogether, 97.5% of the residues in the homology model built were in favored and allowed regions. Comparing with the template, the homology model has a similar Ramachandran plot with a relatively low percentage of residues in general and disallowed distribution (2.5%).

ERRAT is a so-called "overall quality factor" for non-bonded atomic interactions, and higher scores mean higher quality [33]. The normally accepted range is > 50 for a high quality model [33]. In our case, the ERRAT score for the model is 83.2, well within the range of a high quality model; whilethe ERRAT score for the template is 96.7 (Table 1). Thus, the above analysis suggests that the backbone conformation and non-bonded interactions of the homology model are all reasonable and within a normal range.

The normality of the local environment of the homology model was further checked by WHAT-IF. For the WHAT-IF evaluation, the quality of the distribution of atom types is determined around amino fragments [35], and the WHAT-IF packing scores above −5.0 represents a reliable structure. In this case, none of residues has the score lower than −5.0 as depicted in Fig. 7. Therefore, the WHAT-IF evaluation also indicates that the homology mode structure is very reasonable.

The residue interaction energy and the PROSA Z-score was also calculated by the PROSA2003 program [59]. In this analysis, the interaction energy of each residue with the remainder of a protein is calculated to judge whether it fulfills certain energy criteria or not. The PROSA2003 pair energy profiles calculated for the homology model along with the template are depicted in Fig. 8. The C^{α} and C^{β} potential profiles of the homology model are consistent with a reliable conformation based on its similarity with that of the template. The *Z*-score indicates overall model quality and evaluates the deviation of the total energy of the protein structure with respect to an energy distribution derived from random conformations [59]. Specifically, the combined Z-score for the homology model is −3.16, while it is −2.90 for the template. Such results show a similar energy profile for the homology model when compared with the template.

Discrete optimized protein energy (DOPE) is a statistical potential for the assessment of protein models [36] and computes the energy of the tertiary structure of a protein as the sum of the energy for pairs of atoms in the protein. Herein the DOPE results confirm again that a reasonable model was obtained, with an energy score comparable to that of the template (−42396.1 for the model and −42501.6 for the template, respectively).

In summary, several validation criteria, including the geometric quality of the backbone conformation, the residue interaction and the energy profile of the structure, are all well within the limits associated with a high-quality structure. All evidence suggests that a reliable model for α_{1A}-AR has been obtained for further examination of protein-ligand interactions.

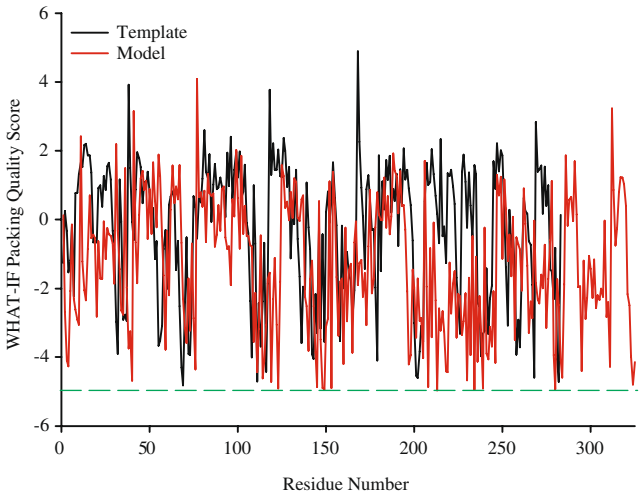

Fig. 7 The WHAT-IF packing quality scores calculated for the template and the homology model. The score should be above −5 for a reliable model

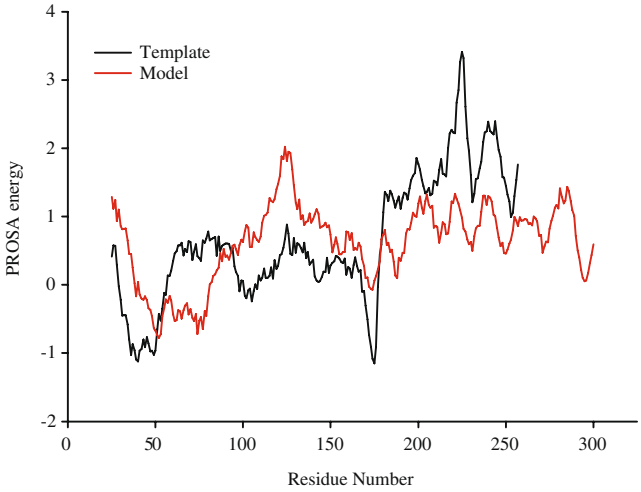

Fig. 8 PROSA2003 pair energy profiles calculated for the template and the homology model. Potentials for both C^{α} and C^{β} interactions were used. The graphs are smoothed over a window size of 50 residues

As a further quality check, we were interested in examining whether we can predict the correct ligand binding profiles of known antagonists reported in the literature by using the homology model built. Therefore, the binding modes of three known subtype-selective α_{1A}-AR antagonists, Silodosin, RWJ-69736 and (+)SNAP-7915 were studied. The compounds were docked into the binding site using DOCK 5.4 [48]. MD simulations were then conducted on these ligand-receptor complexes. Before comparing the docking poses with experimental results, it is important to summarize the general features of the receptor as have been reported based on experimental results. The human α_{1A}-AR consists of 466 amino acids. Based on mutagenesis studies, two phenylalanine residues in transmembrane domain 7 (TM7) (Phe308 and 312), one phenylalanine residue in TM5 (Phe193), and one leucine residue in TM6 (Leu290) have been identified as major contributors to ligand binding by π-stacking and/or hydrophobic interactions [60–62]. Based on alanine-substitution mutation

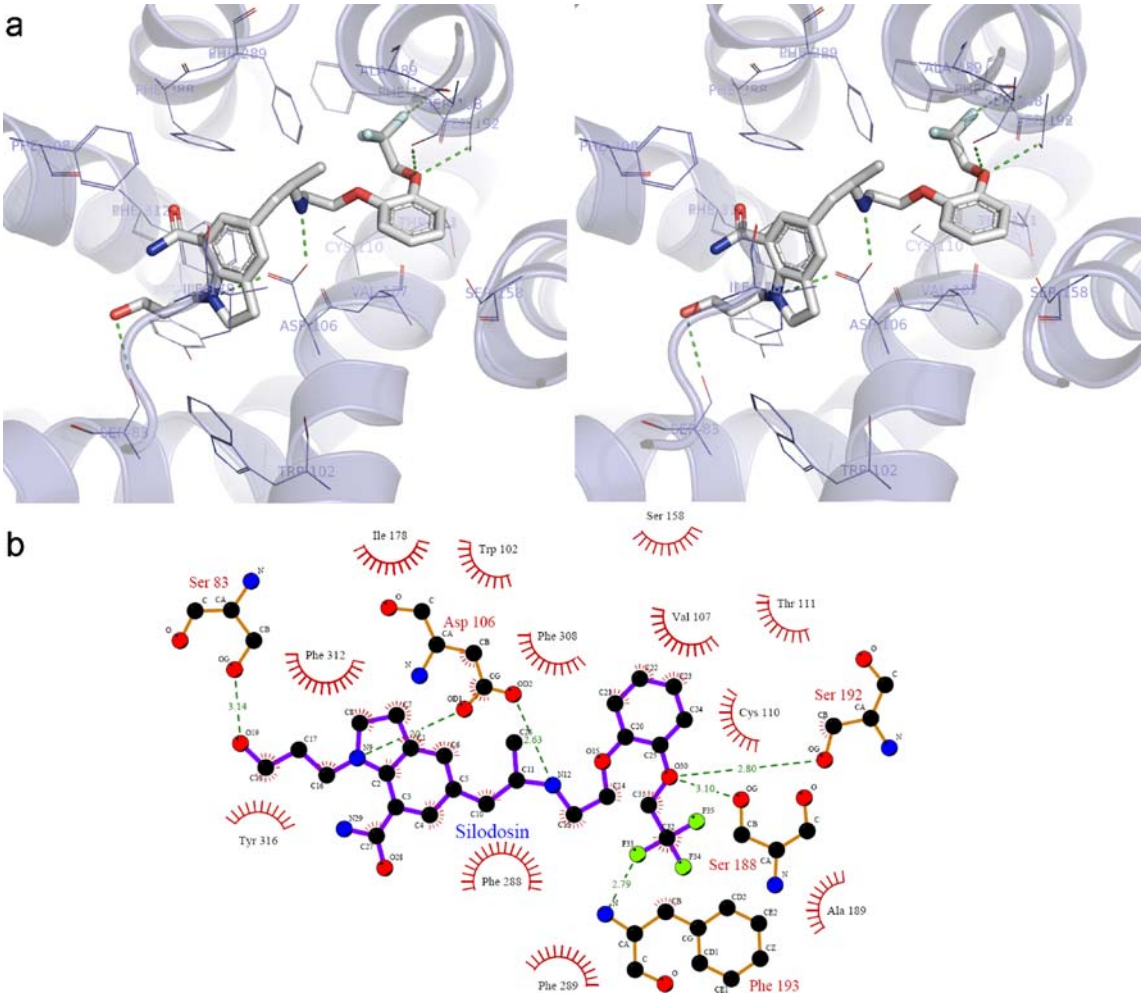

Fig. 9 Proposed stereoscopic docking conformation of silodosin (white sticks) in the human α_{1A}-AR binding site (**a**) and the proposed schematic interactions of silodosin with human α_{1A}-AR (**b**)

experiments, two serine residues in TM5, Ser188 and 192, have been suggested to interact with ligands through hydrogen bond formation [63]. Mutagenesis studies have also indicated that the protonated nitrogen of the bound ligand engages in ionic interactions with an aspartate residue in TM3 (Asp106) [64].

The docking conformation and interaction diagram of Silodosin are depicted in Fig. 9. Asp106 seems to play a key role in antagonist binding through strong electrostatic interactions with the protonated amino group. The indole system seems to engage in strong π-stacking and/or hydrophobic interactions with Trp102, Ile178, Phe288, Phe308, Phe309, Phe312 and Tyr316, while the phenyloxy moiety is inserted into a hydrophobic pocket lined by Val107, Cys110, Tyr111, Ser158, Ala189, Phe193 and Phe289. The docking results also suggest that the nitrogen and hydroxyl groups on the indole propanol portion possibly interact with Asp106 and Ser83 by hydrogen bond formation. Moreover, the trifluoroethoxyl group on the phenyloxy ring is in the right position to form hydrogen bonds with Ser188, Ser192 and Phe193. These proposed functional group interactions, especially those involving Asp106 in TM3, Ser188, Ser192 and Phe193 in TM5, and Phe308 and Phe312 in TM7, are consistent with the results of mutagenesis studies [60, 61, 63, 64].

Figure 10 shows the proposed main interactions between α_{1A}-AR and RWJ-69736. In the proposed binding mode, the carboxylate group of Asp106 engages in ionic interactions with the protonated amino group on the piperazine moiety. The hydroxyl groups of Ser188 and Ser192 form a network of hydrogen bonds with the oxygen atom on the isopropoxy group. Val107, Cys110, Thr111, Ile157, Tyr184, Phe193, Phe288, Phe308, Lys309 and Phe312 line a hydrophobic region that interacts with the major RWJ-69736 scaffold. The above-mentioned interactions are also consistent with mutagenesis results that suggested the

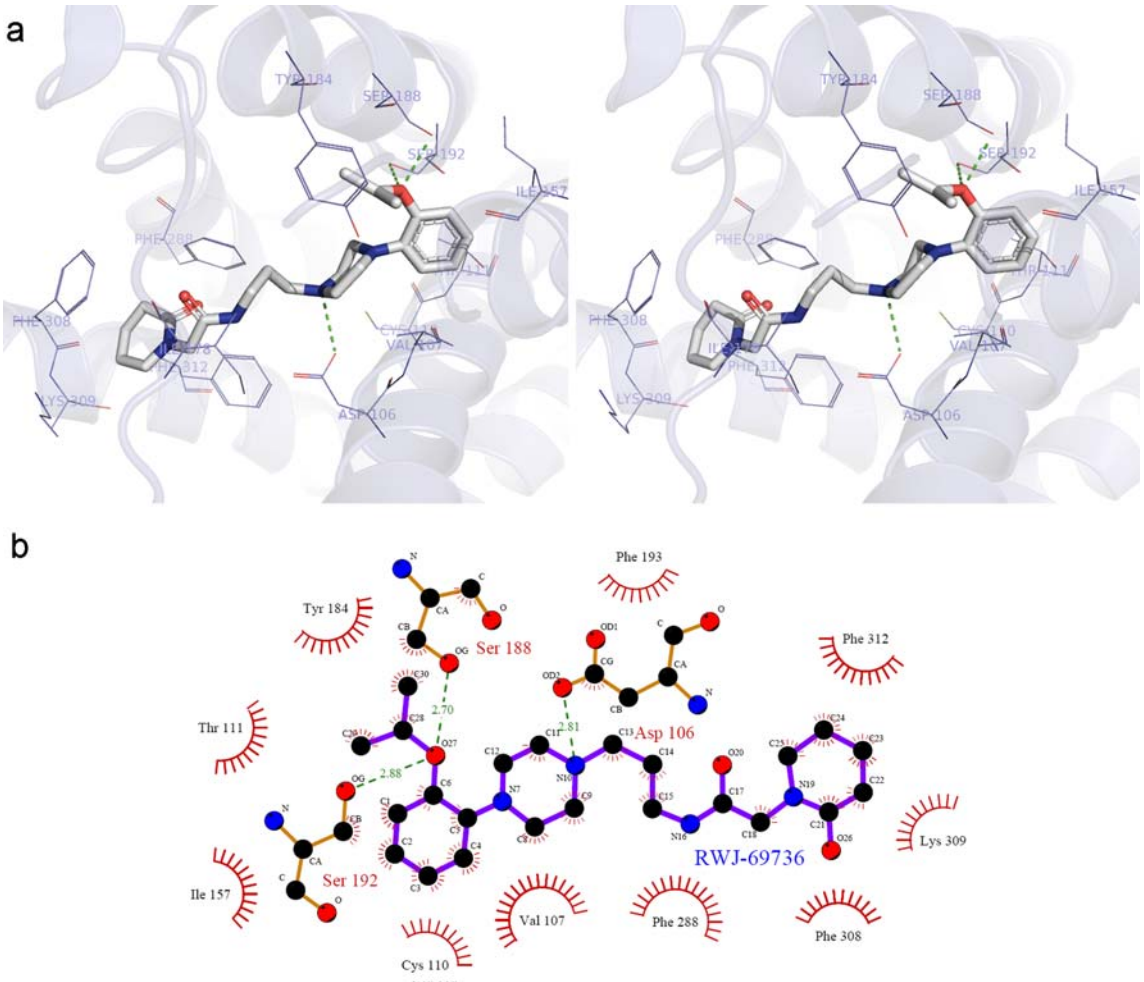

Fig. 10 Proposed stereoscopic docking conformation of RWJ-69736 (white sticks) in the human α_{1A}-AR binding site (**a**) and the proposed schematic interactions of RWJ-69736 with human α_{1A}-AR (**b**)

importance of several residues in binding interactions. These residues include Asp106 in TM3, Ser188, Ser192 and Phe193 in TM5, and Phe308 and Phe312 in TM7 [60, 61, 63, 64]. A few other residues, such as Val107, Cys110, Thr111, Ile157, Tyr184 and Phe288 are also proposed to interact with the antagonists, although these interactions have not been identified by experimental studies.

(+)SNAP-7915 showed a similar binding profile with α_{1A}-AR as Silodosin and RWJ-69736 (Fig. 11). Specifically, the protonated nitrogen on the piperidine ring seems to engage in ionic interactions with the carboxylate group of Asp106. The fluorine atom may have hydrogen bond interactions with Arg166. Similarly, the amide group of RWJ-69736 may have hydrogen bond interactions with Ser188 and 192, and the lactone moiety has hydrogen bonds with Ser158 and Ser192. In addition, Val107, Pro161, Ile178, Tyr184, Phe288, Phe289, Phe308 and Phe312 are clustered together to form a hydrophobic pocket for binding with SNAP-7915. This proposed interaction profile is again in agreement with the mutagenesis data reported in the literature [60, 61, 63, 64].

Overall, results of the docking studies using Silodosin, RWJ-69736 and (+)SNAP-7915 correlate very well with experimental data from mutagenesis studies. Some common patterns involved in antagonist binding are readily apparent from the homology model built: (1) the protonated amine of α_{1A}-AR antagonists can interact with an aspartate residue (Asp106) in TM3; (2) hydrogen bond acceptors/donors on the scaffold of α_{1A}-AR antagonists can interact with two serine residues (Ser188 and 192) in TM5; (3) the lipophilic moiety of α_{1A}-AR antagonists can have hydrophobic and/or π-stacking interactions with some phenylalanine residues, such as Phe193 in TM5 and Phe308 and Phe312 in TM7. The consistency between mutagenesis results and the predicted binding modes of known antagonists suggests that the homology model is of high quality.

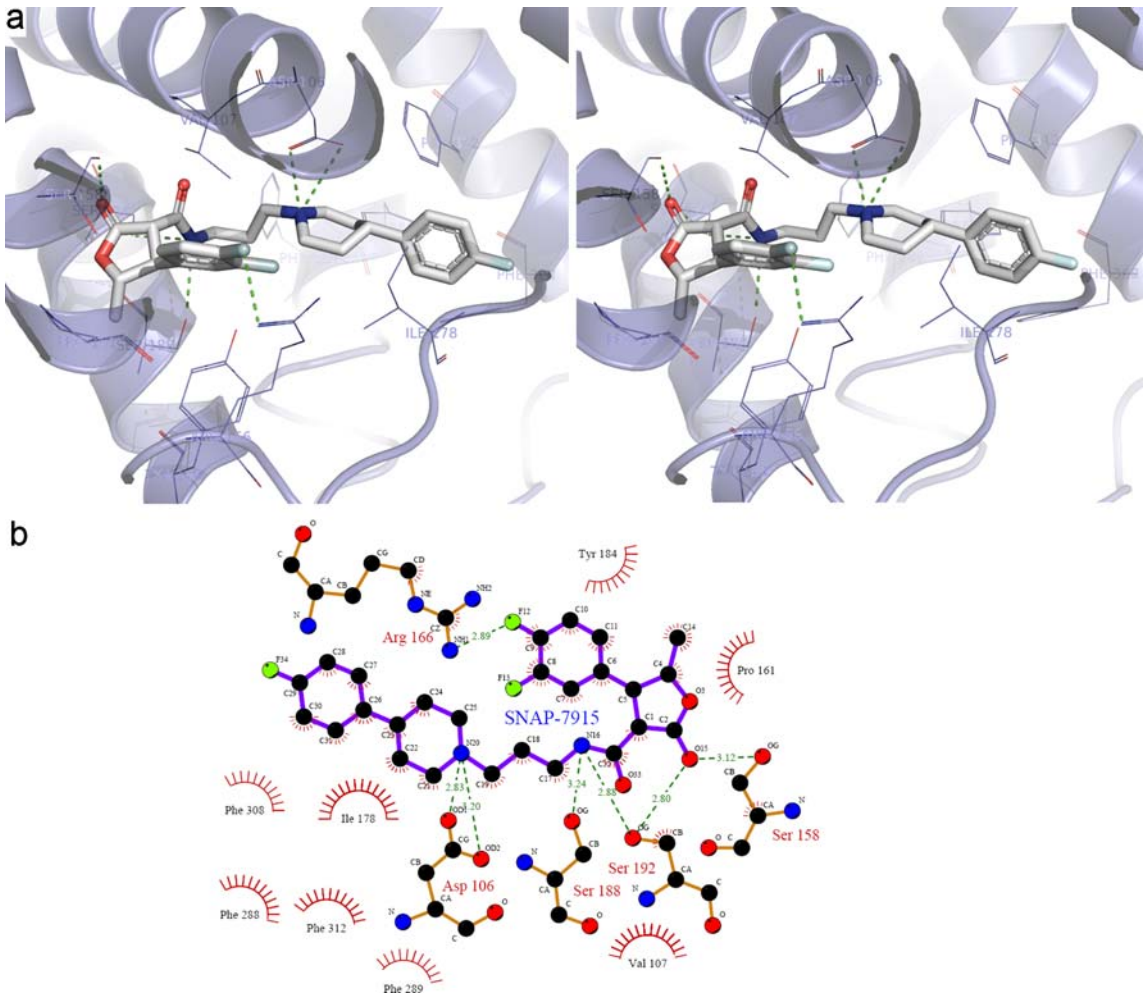

Fig. 11 Proposed stereoscopic docking conformation of SNAP-7915 (white sticks) in the human α_{1A}-AR binding site (**a**) and the proposed schematic interactions of SNAP-7915 with human α_{1A}-AR (**b**)

Conclusions

Though a large number of experimental studies on GPCRs have been conducted, knowledge of how known antagonists bind to α_{1A}-AR remains sketchy. In order to achieve a good level of understanding of the three-dimensional structures of α_{1A}-AR, a rough homology model was firstly developed for human α_{1A}-AR based on the β_2-AR crystal structure, and then optimized by MM and MD simulations using the GBSW implicit membrane model. After evaluation through PROCHECK, ERRAT, VERIFY-3D, WHAT-IF, PROSA2003 and DOPE, the refined model possesses high geometric quality and a good energy profile. In the next step, this model was used in combined docking and molecular dynamics studies to obtain the binding site and binding poses of several known antagonists. The residues involved in binding interactions identified in the homology model are qualitatively consistent with available mutagenesis data. These residues include Asp106 in TM3, Ser188, Ser192 and Phe193 in TM5, and Phe308 and Phe312 in TM7. This α_{1A}-AR homology model should be very useful for guiding further medicinal chemistry work and mutagenesis studies.

Acknowledgements We acknowledge the financial support by China's National 863 Plan (Grant No. 2002AA2Z3118) and the Changjiang Scholarship program of the Ministry of Education, China, Georgia Research Alliance, and Georgia Cancer Coalition.

References

1. Bylund DB, Eikenberg DC, Hieble JP, Langer SZ, Lefkowitz RJ, Minneman KP, Molinoff PB, Ruffolo RR Jr, Trendelenburg U (1994) Pharmacol Rev 46:121–136
2. Hieble JP, Bylund DB, Clarke DE, Eikenburg DC, Langer SZ, Lefkowitz RJ, Minneman KP, Ruffolo RR (1995) Pharmacol Rev 47:267–270
3. Zhong H, Minneman KP (1999) Eur J Pharmacol 375:261–276
4. Hawrylyshyn KA, Michelotti GA, Coge F, Guenin SP, Schwinn DA (2004) Trends Pharmacol Sci 25:449–455
5. Andersson KE (2002) World J Urol 19:390–396
6. Li MY, Du LP, Wu B, Xia L (2003) Bioorg Med Chem 11:3945–3951
7. Li MY, Lu JF, Xia L (2005) Acta Chim Sinica 63:1875–1883
8. Li MY, Fang H, Xia L (2005) Bioorg Med Chem Lett 15:3216–3219
9. Fang H, Li MY, Xia L (2007) Chinese Chem Lett 18:41–44
10. Fang H, Li MY, Xia L, Jiang ZZ, Lu ZZ (2005) Chinese Chem Lett 16:445–448
11. Wu B, Li MY, Jiang ZZ, Xia L (2004) Chinese J Org Chem 24:1587–1594
12. Wu B, Li MY, Jiang ZZ, Xia L (2004) Acta Chim Sinica 62:1430–1436
13. Li MY, Xia L (2007) Chem Biol Drug Des 70:461–464
14. Ishiguro M, Futabayashi Y, Ohnuki T, Ahmed M, Muramatsu I, Nagatomo T (2002) Life Sci 71:2531–2541
15. Kinsella GK, Rozas I, Watson GW (2004) Biochem Biophys Res Commun 324:916–921
16. Pedretti A, Elena Silva M, Villa L, Vistoli G (2004) Biochem Biophys Res Commun 319:493–500
17. Tramontano A (1998) Methods 14:293–300
18. Cherezov V, Rosenbaum DM, Hanson MA, Rasmussen SG, Thian FS, Kobilka TS, Choi HJ, Kuhn P, Weis WI, Kobilka BK, Stevens RC (2007) Science 318:1258–1265
19. Rosenbaum DM, Cherezov V, Hanson MA, Rasmussen SG, Thian FS, Kobilka TS, Choi HJ, Yao XJ, Weis WI, Stevens RC, Kobilka BK (2007) Science 318:1266–1273
20. Rasmussen SG, Choi HJ, Rosenbaum DM, Kobilka TS, Thian FS, Edwards PC, Burghammer M, Ratnala VR, Sanishvili R, Fischetti RF, Schertler GF, Weis WI, Kobilka BK (2007) Nature 450:383–387
21. Kobilka B, Schertler GF (2008) Trends Pharmacol Sci 29:79–83
22. Ginalski K (2006) Curr Opin Struct Biol 16:172–177
23. Notredame C, Higgins DG, Heringa J (2000) J Mol Biol 302:205–217
24. Gouet P, Robert X, Courcelle E (2003) Nucleic Acids Res 31:3320–3323
25. Fiser A, Sali A (2003) Methods Enzymol 374:461–491
26. Brooks BR, Bruccoleri RE, Olafson BD, States DJ, Swaminathan S, Karplus M (1983) J Comput Chem 4:187–217
27. Im W, Feig M, Brooks CL (2003) Biophys J 85:2900–2918
28. Jo S, Kim T, Im W (2007) PLoS ONE 2:e880
29. MacKerell AD, Bashford D, Bellott M, Dunbrack RL, Evanseck JD, Field MJ, Fischer S, Gao J, Guo H, Ha S, Joseph-McCarthy D, Kuchnir L, Kuczera K, Lau FTK, Mattos C, Michnick S, Ngo T, Nguyen DT, Prodhom B, Reiher WE, Roux B, Schlenkrich M, Smith JC, Stote R, Straub J, Watanabe M, Wiorkiewicz-Kuczera J, Yin D, Karplus M (1998) J Phys Chem B 102:3586–3616
30. Ryckaert J-P, Ciccotti G, Berendsen HJC (1977) J Comput Phys 23:327–341
31. Kleywegt GJ (2000) Acta Crystallogr D Biol Crystallogr 56:249–265
32. Laskowski RA, Rullmannn JA, MacArthur MW, Kaptein R, Thornton JM (1996) J Biomol NMR 8:477–486
33. Colovos C, Yeates TO (1993) Protein Sci 2:1511–1519
34. Eisenberg D, Luthy R, Bowie JU (1997) Methods Enzymol 277:396–404
35. Vriend G, Sander C (1993) J Appl Cryst 26:47–60
36. Shen MY, Sali A (2006) Protein Sci 15:2507–2524
37. Du LP, Li MY, Tsai KC, You QD, Xia L (2005) Biochem Biophys Res Commun 332:677–687
38. Du LP, Li MY, You QD, Xia L (2007) Biochem Biophys Res Commun 355:889–894
39. Li MY, Wang BH (2007) J Mol Model 13:1237–1244
40. Yang Q, Du L, Wang X, Li M, You Q (2008) J Mol Graph Model doi:10.1016/j.jmgm.2008.04.002
41. Yoshida M, Homma Y, Kawabe K (2007) Expert Opin Investig Drugs 16:1955–1965
42. Pulito VL, Li X, Varga SS, Mulcahy LS, Clark KS, Halbert SA, Reitz AB, Murray WV, Jolliffe LK (2000) J Pharmacol Exp Ther 294:224–229
43. Lagu B, Tian D, Jeon Y, Li C, Wetzel JM, Nagarathnam D, Shen Q, Forray C, Chang RS, Broten TP, Ransom RW, Chan TB, O'Malley SS, Schorn TW, Rodrigues AD, Kassahun K, Pettibone DJ, Freidinger RO, Gluchowski C (2000) J Med Chem 43:2775–2778
44. Stewart JJ (1990) J Comput Aided Mol Des 4:1–105
45. Jakalian A, Bush BL, Jack DB, Bayly CI (2000) J Comput Chem 21:132–146
46. Jakalian A, Jack DB, Bayly CI (2002) J Comput Chem 23:1623–1641
47. Tsai K-C, Wang S-H, Hsiao N-W, Li M, Wang B (2008) Bioorg Med Chem Lett 18:3509–3512
48. Moustakas DT, Lang PT, Pegg S, Pettersen E, Kuntz ID, Brooijmans N, Rizzo RC (2006) J Comput Aided Mol Des 20:601–619

49. McDonald IK, Thornton JM (1994) J Mol Biol 238:777–793
50. Wallace AC, Laskowski RA, Thornton JM (1995) Protein Eng 8:127–134
51. DeLano WL (2006) The PyMOL molecular graphics system, 0.99; DeLano Scientific, San Carlos, CA, USA
52. Krieger E, Nabuurs SB, Vriend G (2003) Methods Biochem Anal 44:509–523
53. Patny A, Desai PV, Avery MA (2006) Curr Med Chem 13:1667–1691
54. Ginalski K (2006) Curr Opin Struct Biol 16:172–177
55. Xiang Z (2006) Curr Protein Pept Sci 7:217–227
56. Forrest LR, Tang CL, Honig B (2006) Biophys J 91:508–517
57. Mehler EL, Periole X, Hassan SA, Weinstein H (2002) J Comput Aided Mol Des 16:841–853
58. Kandt C, Ash WL, Tieleman DP (2007) Methods 41:475–488
59. Tomii K, Hirokawa T, Motono C (2005) Proteins 61(Suppl 7):114–121
60. Waugh DJ, Gaivin RJ, Zuscik MJ, Gonzalez-Cabrera P, Ross SA, Yun J, Perez DM (2001) J Biol Chem 276:25366–25371
61. Wetzel JM, Salon JA, Tamm JA, Forray C, Craig D, Nakanishi H, Cui W, Vaysse PJ, Chiu G, Weinshank RL, Hartig PR, Branchek TA, Gluchowski C (1996) Recept Channels 4:165–177
62. McCune D, Gaivin R, Rorabaugh B, Perez D (2004) Recept Channels 10:109–116
63. Hwa J, Perez DM (1996) J Biol Chem 271:6322–6327
64. Perez DM (2007) Biochem Pharmacol 73:1051–1062